

Calibrating the scintillation and ionization responses of xenon recoils for high-energy dark matter searches

LIDINE 2022
September 22nd, 2022

[arXiv 2207.08326](https://arxiv.org/abs/2207.08326)
Accepted to Phys. Rev. D

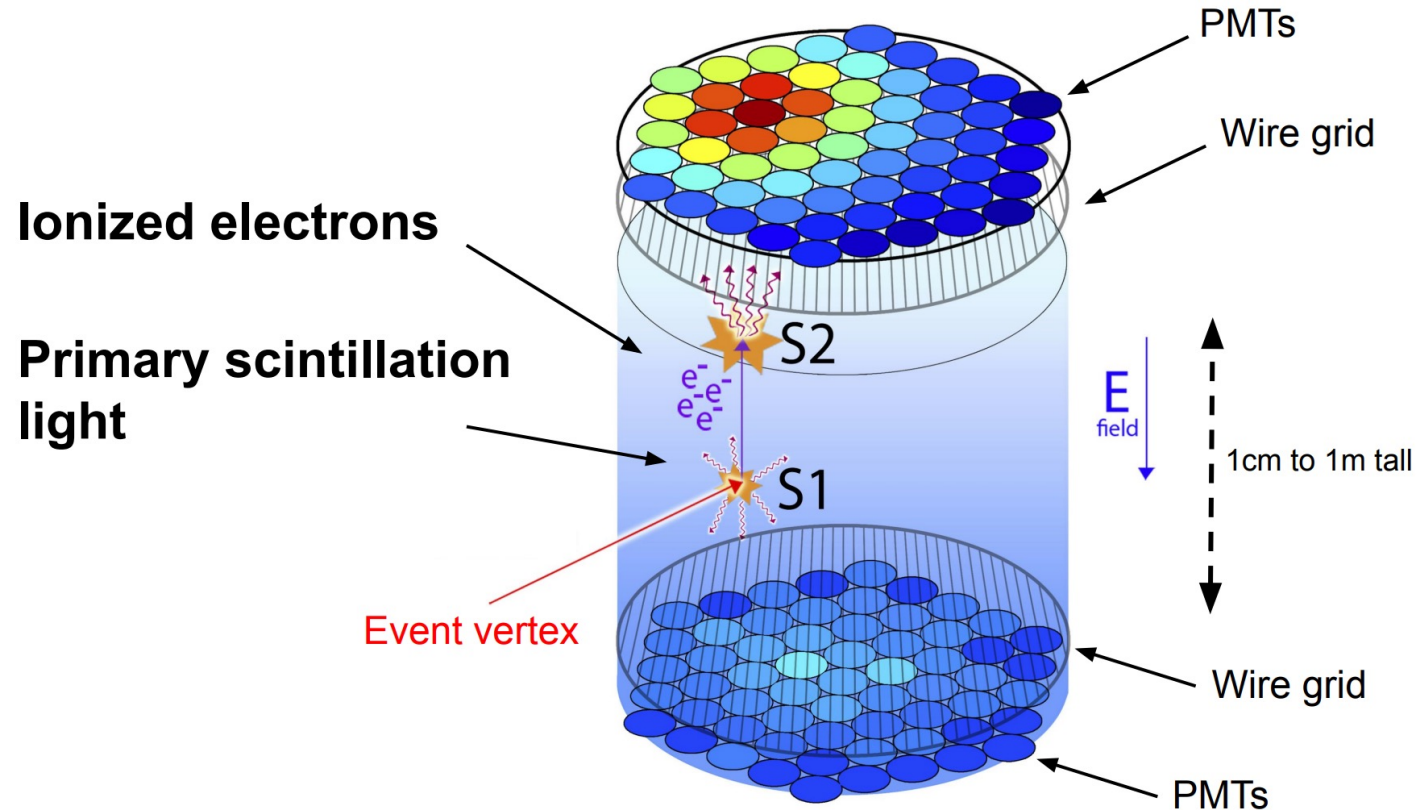
Speaker: Teal Pershing (LLNL)

Contributing authors: Daniel Naim, Brian Lenardo, Jingke Xu, James Kingston, Eli Mizrachi, Vladimir Mozin, Phillip Kerr, Sergey Pereverzev, Adam Bernstein, Mani Tripathi



Detecting particle interactions in Xenon TPCs

Figure by CH Faham (Brown)

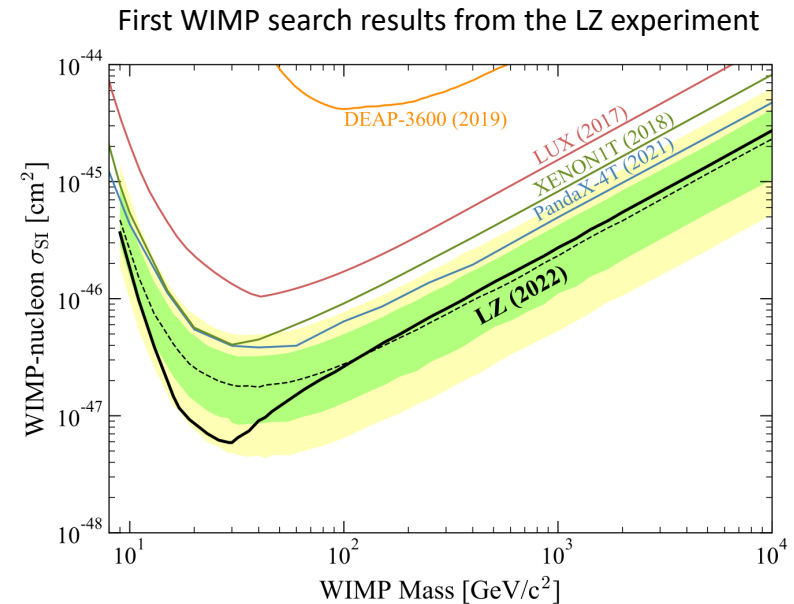
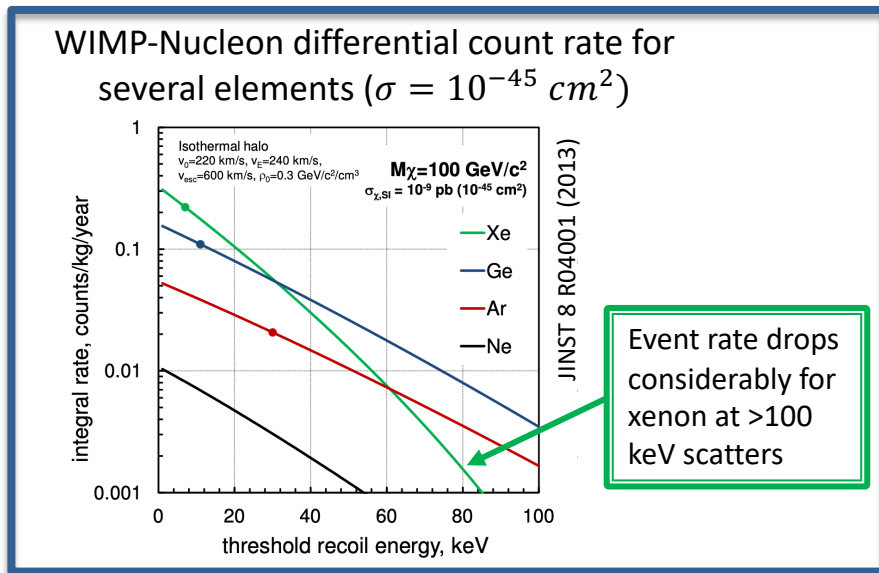


Event vertex

- ionization electrons Charge yield
- UV scintillation photons (~175 nm) Light yield

Dark matter searches using Xenon TPCs

- Most WIMP dark matter searches with xenon TPCs have optimized searches on neutron recoil energy signatures predicted by canonical dark matter models (<100 keV regime)
 - So far, no detection of a WIMP signal in the commonly searched region

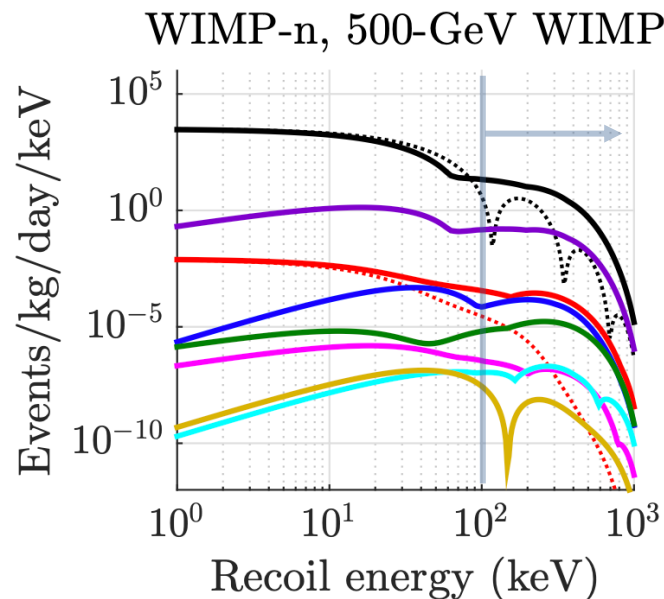


Expanding the search window for WIMP recoils

- Can test aspects of models predicting higher energy nuclear recoils
 - Some couplings in effective field theories suppressed at lower recoil energies
 - Inelastic WIMP scatters can result in higher energy signals
- Room to improve sensitivity for higher mass WIMPs in canonical models
 - Merit in searching for signatures of dark matter in less-explored ranges

- \mathcal{O}_1 , M , $\sim q^0$
-Standard SI
- \mathcal{O}_4 , $\Sigma'' + \Sigma'$, $\sim q^0$
-Standard SD
- \mathcal{O}_3 , Σ' and Φ'' , $\sim q^2$
- \mathcal{O}_5 , M and Δ , $\sim q^2$
- \mathcal{O}_6 , Σ'' , $\sim q^4$
- \mathcal{O}_9 , Σ' , $\sim q^2$
- \mathcal{O}_{11} , M , $\sim q^2$
- \mathcal{O}_{13} , Σ'' and $\tilde{\Phi}'$, $\sim q^2$

arXiv:2102.06998

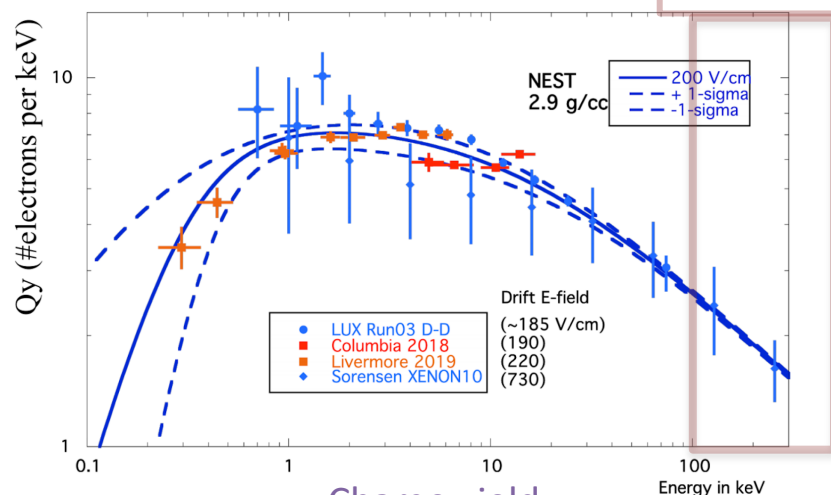
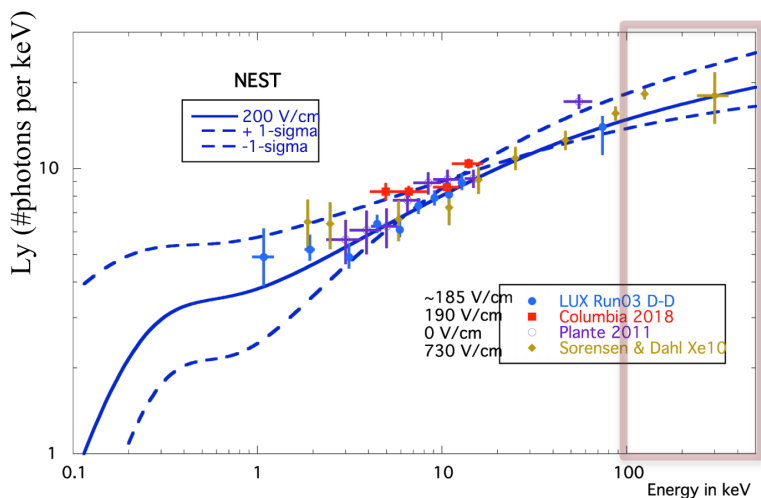


Interaction rates for couplings predicted in effective field theory framework go to higher recoil energies

Characterizing light and charge yield of xenon recoils

- Light and charge yield calibrations inform what S1/S2 sizes are expected from nuclear recoils at different energies
- Additional higher energy calibrations (>100 keV) would help reduce uncertainties associated with event reconstruction
- Also need these yields at different drift field strengths to study field dependence

Summary of current light/charge yield measurements in xenon



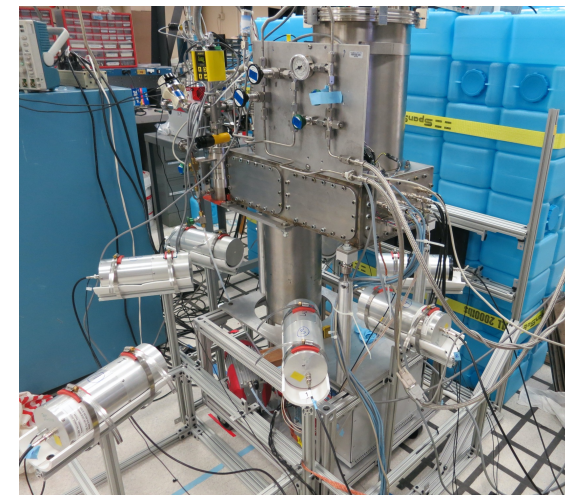
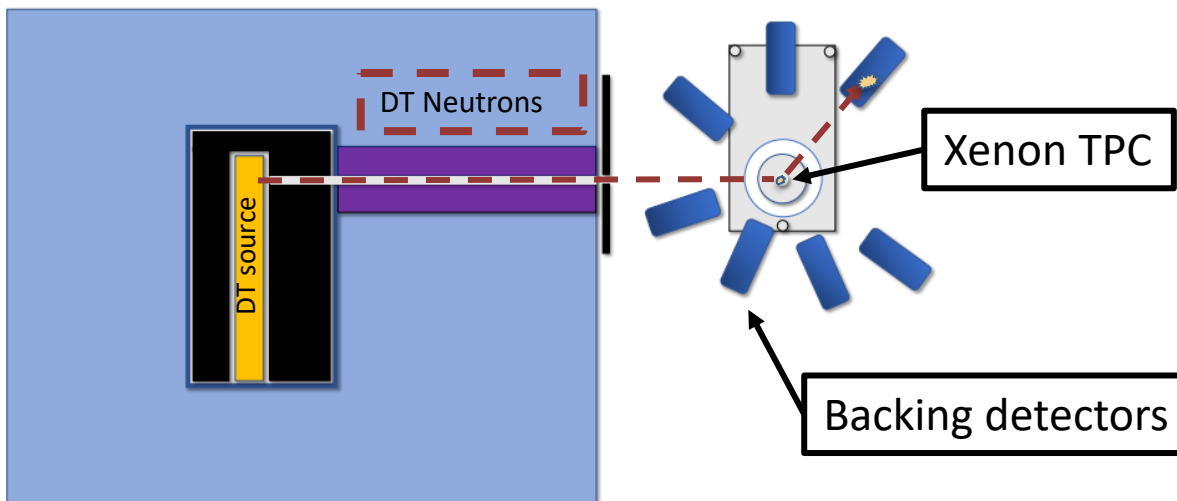
More data needed!

Light yield

Charge yield

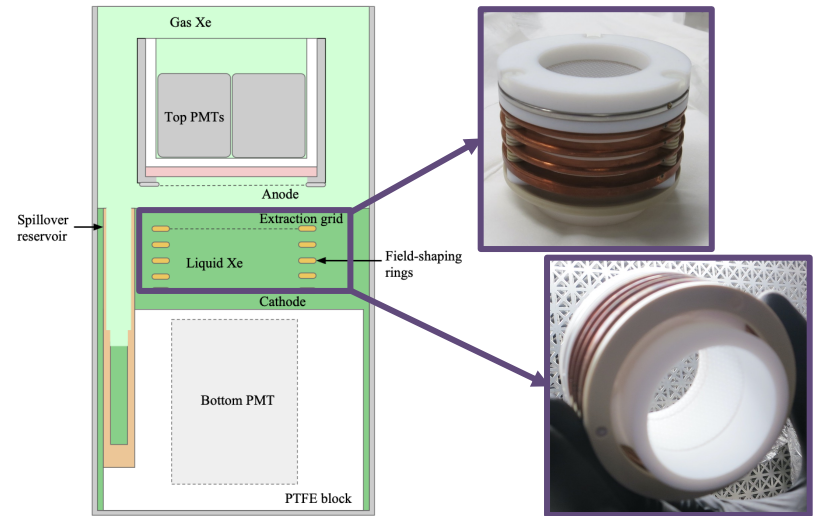
The XeNu DT measurement at LLNL

- Collimated monoenergetic (14.1 MeV) beam used to generate nuclear recoils
 - Energy endpoint for neutron elastic scatters: 430 keV
- Coincident pulse in a Backing Detector (BD) used to reconstruct scattering angle/energy
 - Seven BDs used to tag scatters associated with different recoil energies
- DT source operated at $4.7E7$ neutrons/sec for a total of 40 hours
 - Neutron recoils characterized at three different drift fields

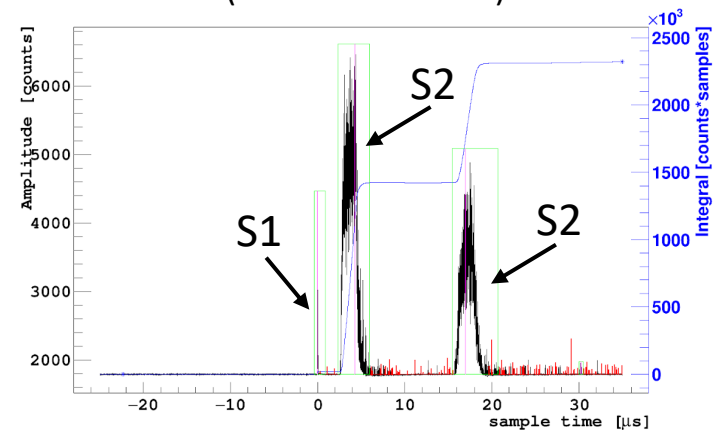


The XeNu Detector

- Dual-phase TPC
 - 150 g active xenon (5 cm diam., 2.5 cm. high)
 - Top: Four 1" Hamamatsu R8520-406 PMTs
 - Bottom: One 2" Hamamatsu R8778 PMT
- High reflectivity PTFE lines active volume to increase S1 light yield
 - Improves NR/ER discrimination, time-of-flight estimation, and precisely measuring the S1 light yield
- Field in electron drift and extraction fields are independently tunable
 - Data collected at three drift fields to characterize field dependence of yields
 - 200 V/cm
 - 760 V/cm
 - 2000 V/cm

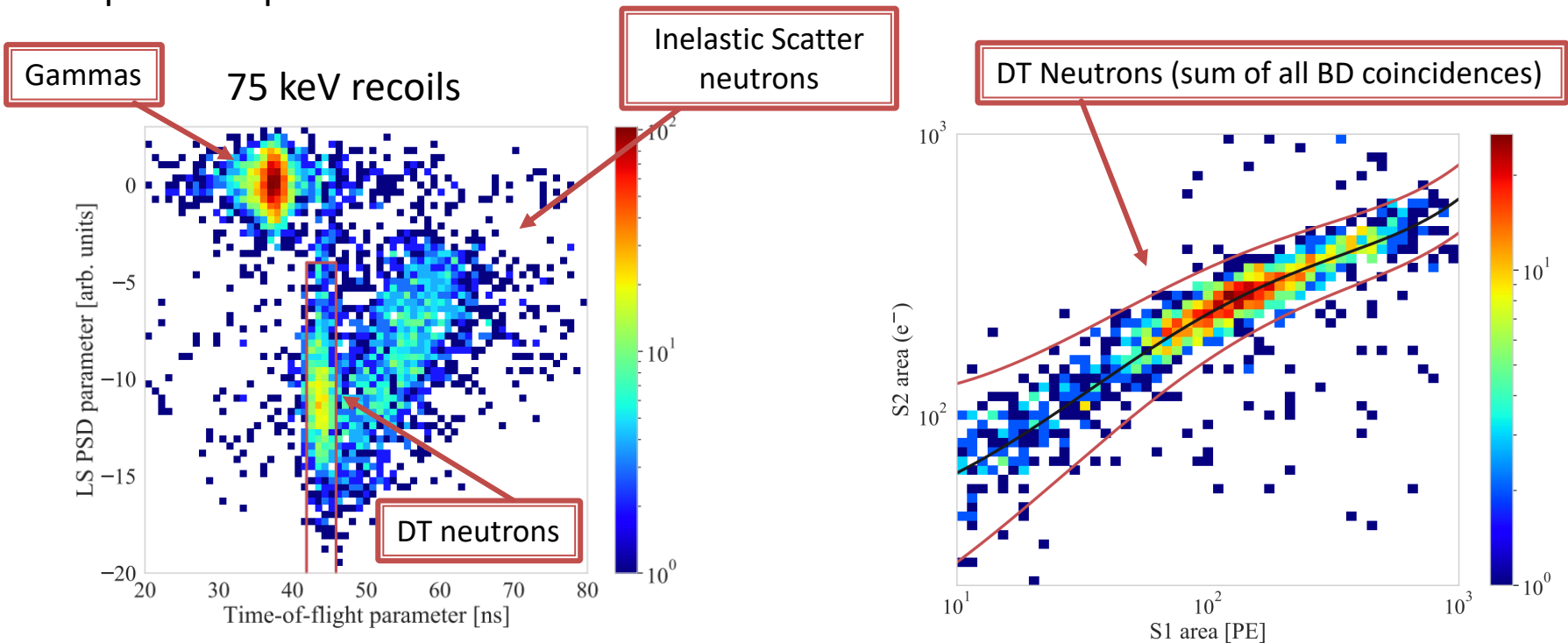


Multi-scatter event in XeNu
(60-Co calibration)



Neutron elastic scatter event selection

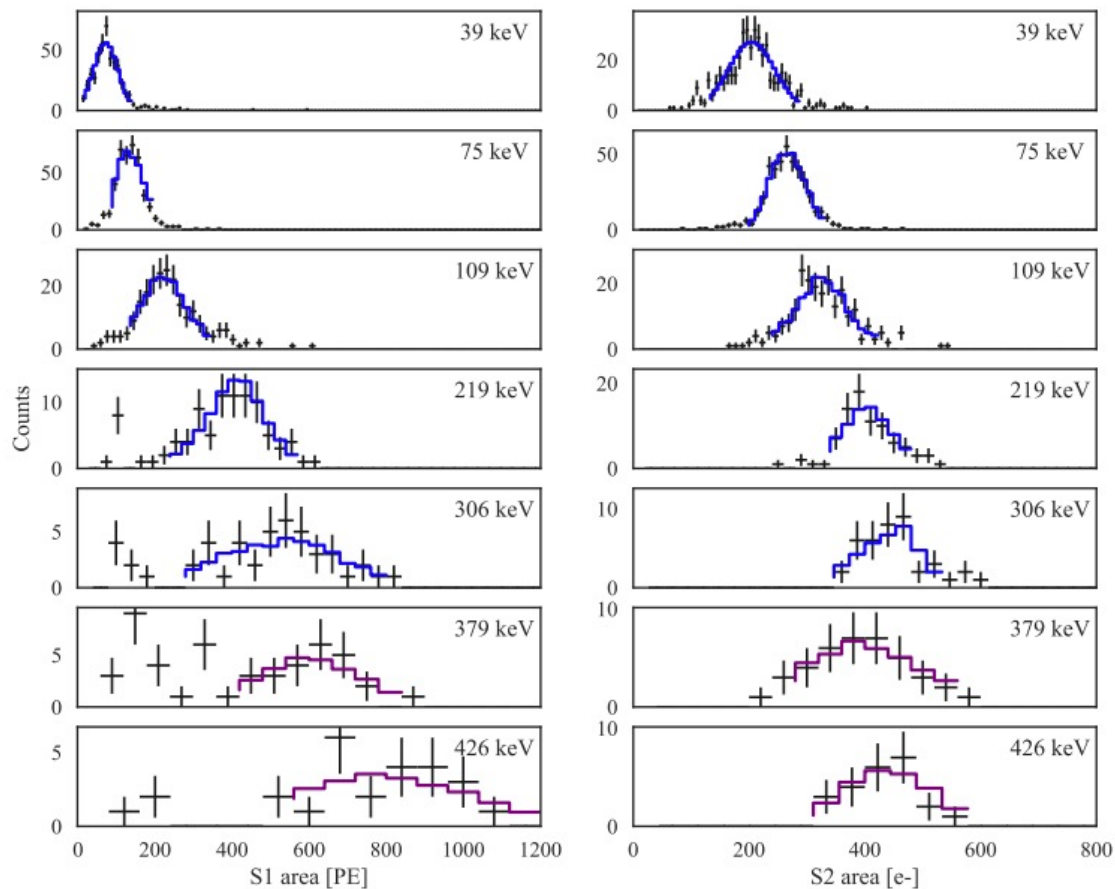
- Several preliminary cuts applied to select neutron elastic scatters
 - Time of flight, LS pulse shape discrimination, Xenon TPC S1/S2 discrimination
- Cuts aggressively remove majority of background gammas and accidentals, providing a pure sample of neutron elastic scatters



Fits to S1/S2 distributions in data

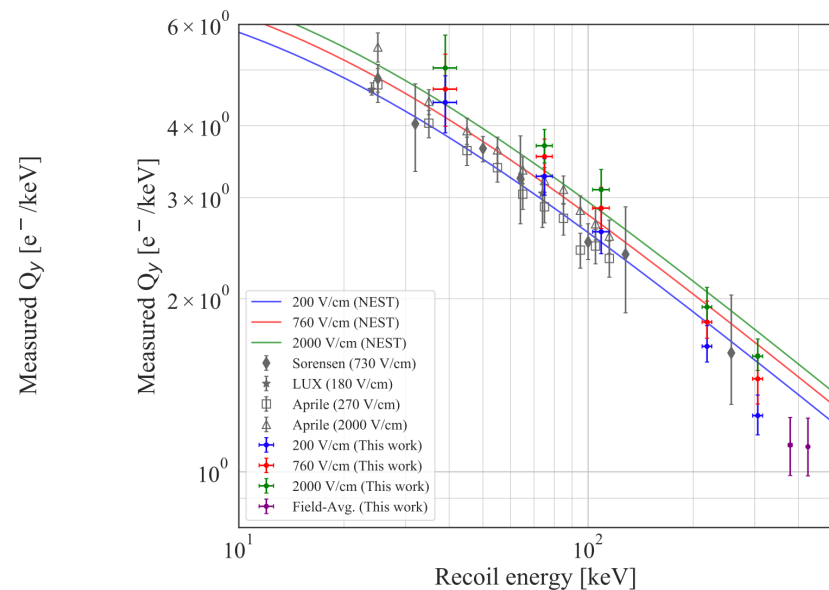
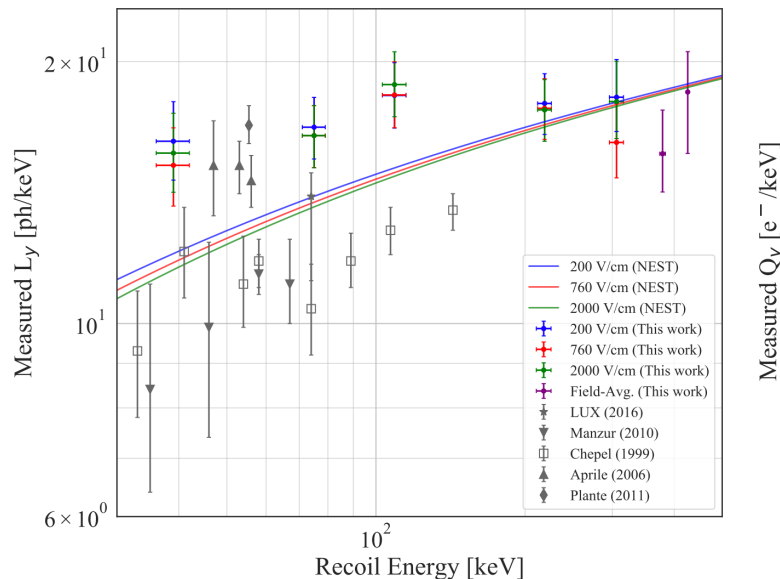
- Model to perform fits to data developed with GEANT4-based simulation of detectors, DT source, and shielding
 - Detector effects and necessary corrections applied to simulated energy distribution to model photon/electron counts
- Light/charge yield values providing the best fit to data estimated using MCMC-based Metropolis-Hastings algorithm
 - Light/charge yield are assumed to locally be a Power law shape near the recoil energy peak
- For higher energies, much lower statistics in peak than expected/predicted by Geant4
 - Due to low statistics, field-averaged values are estimated for the largest recoil energy datasets

Best fits for 2000 V/cm drift field dataset



Preliminary light/charge yield estimates

- Measured charge and light yields shown in comparison to past measurements and predictions from NESTpy v2.3.6
 - Higher values than NEST at <200 keV recoil energies, lower than NEST above 200 keV
- Field dependence of data generally in agreement with predictions in NEST
 - Inconclusive field dependence for light yield due to uncertainties on measurement
 - Charge yield increases as the drift field strength increases



Conclusions

- Nucleon recoil calibrations are needed for Xenon at energies >100 keV to help improve sensitivity to larger energy scattering signatures in dark matter
- A measurement of light/charge yields for nuclear recoils up to 426 keV in energy has been completed
 - Field-dependent yields measured up to 306 keV
 - Field-averaged yields reported at 379 keV and 426 keV due to lower-than-anticipated statistics
- Light/charge yield measurements will be incorporated into NEST following final publication of results



Disclaimer

This document was prepared as an account of work sponsored by an agency of the United States government. Neither the United States government nor Lawrence Livermore National Security, LLC, nor any of their employees makes any warranty, expressed or implied, or assumes any legal liability or responsibility for the accuracy, completeness, or usefulness of any information, apparatus, product, or process disclosed, or represents that its use would not infringe privately owned rights. Reference herein to any specific commercial product, process, or service by trade name, trademark, manufacturer, or otherwise does not necessarily constitute or imply its endorsement, recommendation, or favoring by the United States government or Lawrence Livermore National Security, LLC. The views and opinions of authors expressed herein do not necessarily state or reflect those of the United States government or Lawrence Livermore National Security, LLC, and shall not be used for advertising or product endorsement purposes.

Back-up slides



Developing a model for experimental data

- Full GEANT4-based simulation of detectors, DT source, and shielding
- Preliminary cuts equivalent to those applied in data also applied in simulation
 - Time-of-flight
 - Neutron scatter in backing detector
 - No gamma scatter in xenon TPC
- Detector effects and corrections quantified with calibration data, then applied to simulation using MC techniques to convert to PE/e- counts
 - Light collection efficiency
 - Electron extraction efficiency
 - S1 and S2 drift time dependence corrections

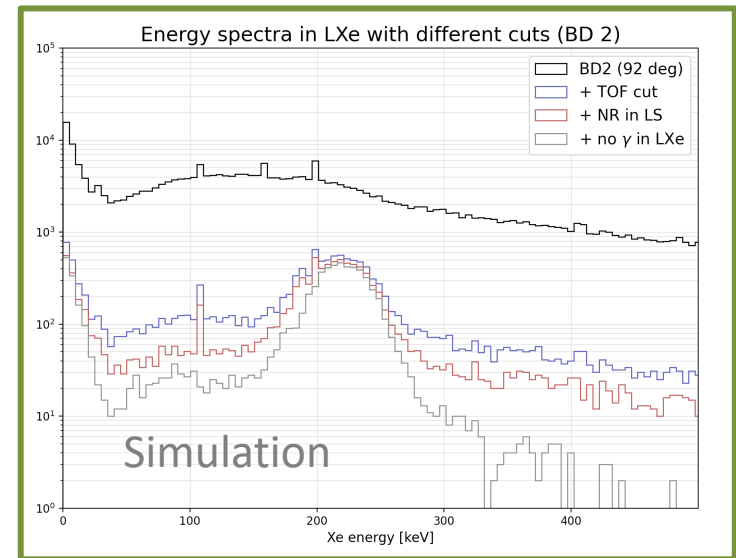
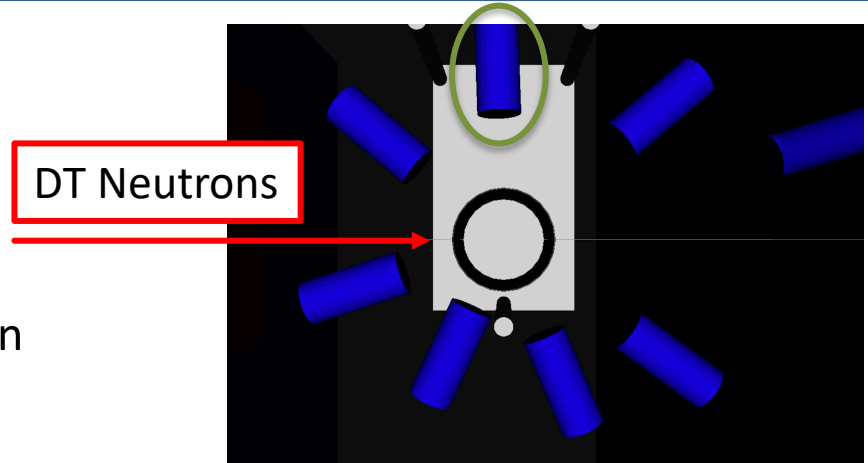


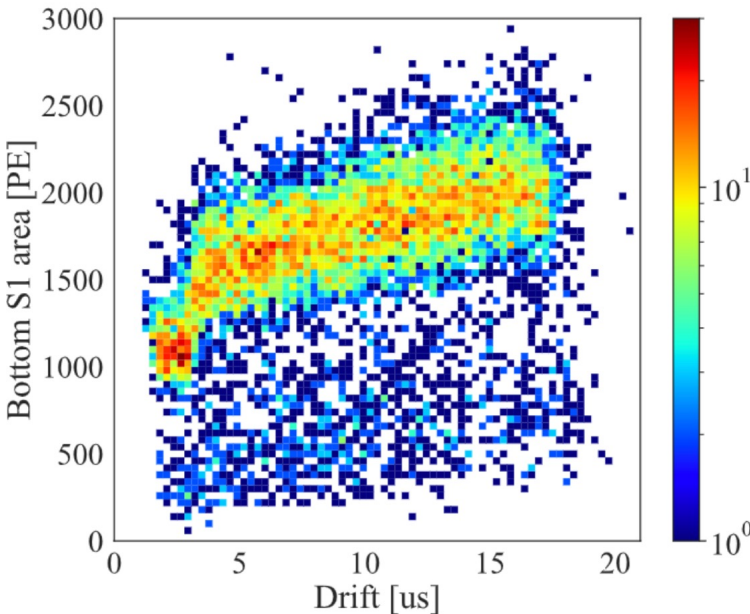
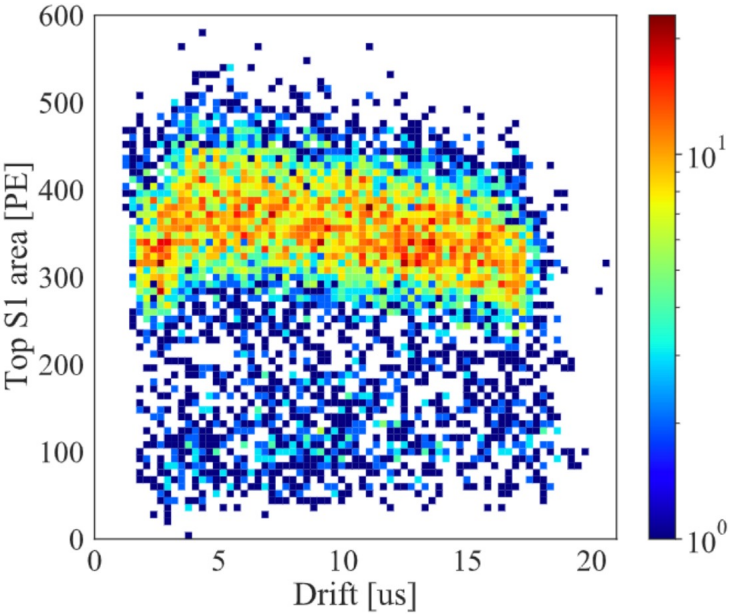
Table of measured values in experiment

- TOF systematic quantifies uncertainty due to (n,2n) contamination of primary DT neutron peak
 - Re-evaluate fits using TOF windows on both sides of the primary DT neutron peak ([-2,0] ns and [0,+2] ns around TOF mean)
- LCE systematic quantified via uncertainty on g1 fit extracted from Doke plot
- EEE systematic uncertainty evaluated for XeNu in previous measurement

scattering angle (deg.)	recoil energy (keV)	Qy					Ly				
		0.2 kV/cm	0.76 kV/cm	2.0 kV/cm	Field avg.	TOF sys.	0.2 kV/cm	0.76 kV/cm	2.0 kV/cm	Field avg.	TOF sys.
36 ± 1	39 ± 3	4.39 ^{+0.23} _{-0.33}	4.63 ^{+0.52} _{-0.50}	5.04 ^{+0.50} _{-0.48}	-	+5.3% -2.7%	16.2 ^{+0.8} _{-0.7}	15.2 ^{+0.5} _{-0.8}	15.7 ^{+0.8} _{-0.7}	-	+5.5% -2.3%
50 ± 1	75 ± 4	3.26 ^{+0.16} _{-0.16}	3.54 ^{+0.17} _{-0.17}	3.69 ^{+0.14} _{-0.14}	-	+1.6% -1.4%	16.8 ^{+0.2} _{-0.2}	16.4 ^{+0.2} _{-0.2}	16.4 ^{+0.3} _{-0.3}	-	+1.9% -1.3%
67 ± 2	109 ± 6	2.62 ^{+0.16} _{-0.16}	2.87 ^{+0.15} _{-0.15}	3.10 ^{+0.15} _{-0.15}	-	+4.3% -2.3%	18.3 ^{+0.5} _{-0.4}	18.3 ^{+0.5} _{-0.5}	18.8 ^{+0.5} _{-0.4}	-	+3.5% -0.5%
92 ± 2	219 ± 7	1.66 ^{+0.08} _{-0.08}	1.82 ^{+0.09} _{-0.10}	1.93 ^{+0.08} _{-0.08}	-	+6.4% -1.8%	17.9 ^{+0.4} _{-0.4}	17.7 ^{+0.3} _{-0.4}	17.6 ^{+0.5} _{-0.4}	-	+2.2% -0.1%
115 ± 3	306 ± 10	1.25 ^{+0.08} _{-0.08}	1.45 ^{+0.13} _{-0.12}	1.59 ^{+0.07} _{-0.07}	-	+2.0% -1.2%	18.2 ^{+0.6} _{-0.5}	16.1 ^{+0.7} _{-0.6}	18.0 ^{+1.0} _{-0.8}	-	+6.4% -3.0%
140 ± 2	379 ± 5	-	-	-	1.12 ^{+0.14} _{-0.14}	+3.1% -2.0%	-	-	-	15.7 ^{+0.9} _{-0.8}	+8.0% -3.1%
162 ± 2	426 ± 2	-	-	-	1.11 ^{+0.14} _{-0.13}	+4.6% -1.2%	-	-	-	18.5 ^{+1.3} _{-1.5}	+4.9% -10.0%
LCE systematic unc.		-					±7.4%				
EEE systematic unc.		±3.0%					-				

Drift time correction applied to S1 data

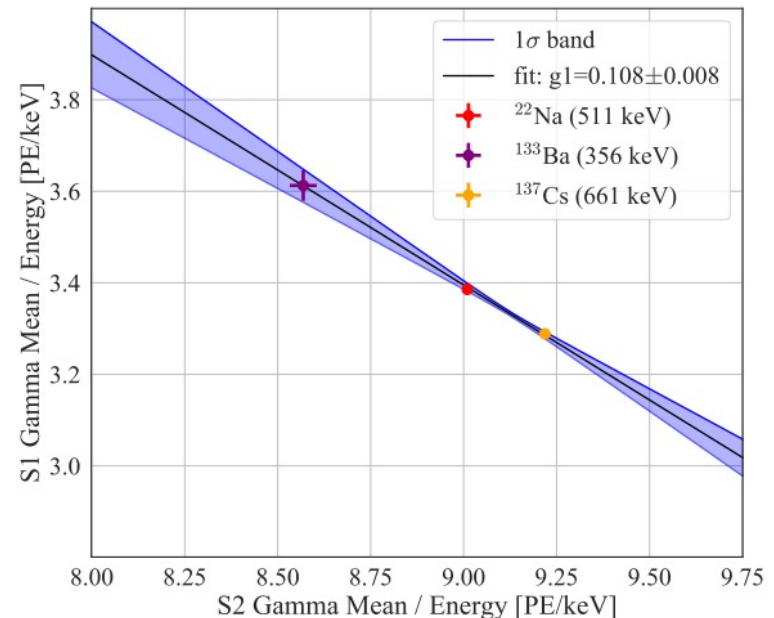
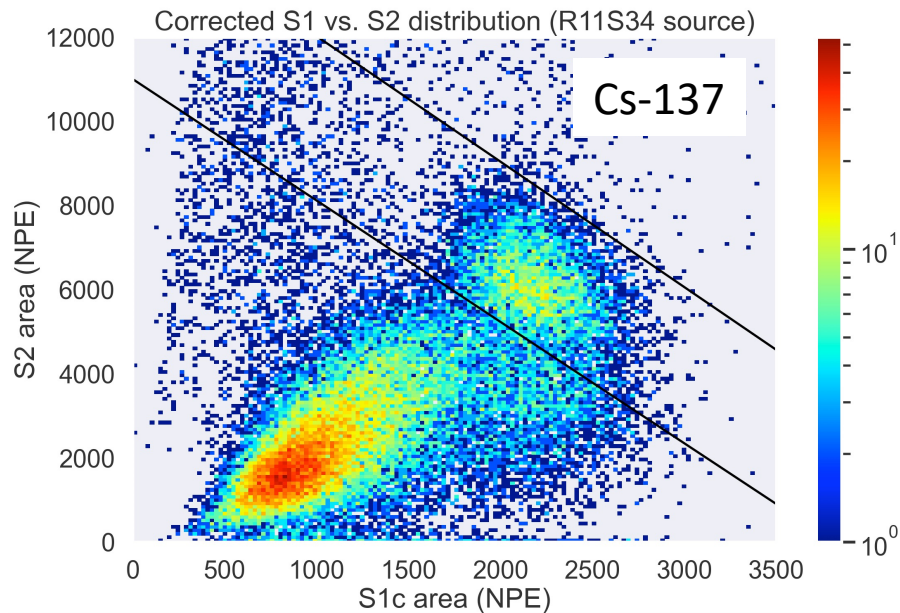
- Collection efficiency of S1 light for top/bottom PMTs is interaction depth-dependent
- Correction applied to top/bottom PMTs to correct S1 area relative to center of TPC



Light Collection Efficiency Measurement

- Fit a 2D Gaussian to the endpoint of several calibration sources
- Then, fit a line on the S1/energy vs. S2/energy space and extract light yield with a line fit

$$E = W(n_{\text{ph}} + n_e) = W_{e/\gamma} \left(\frac{S1}{g1} + \frac{S2}{g2} \right)$$



Collimator and shielding construction

- DT source emits neutrons in all directions
 - Neutrons hitting backing detectors will result in false xenon-BD coincidence signals
 - Neutrons scattering off surrounding environment form backgrounds for neutrons directly from source
- Stand designed for LLNL DT source
 - Lead mounted around source/collimator to reduce mean energy of off-beam neutrons
 - Borated polyethylene and water surrounding source to slow/stop gammas and neutrons
- Entire stand surrounded with borated water for further neutron/gamma shielding
 - 1" collimator formed using borated polyethylene



DT stand frame, anchored



DT stand frame, constructed and partially shielded



Neutron collimator



DT source cave

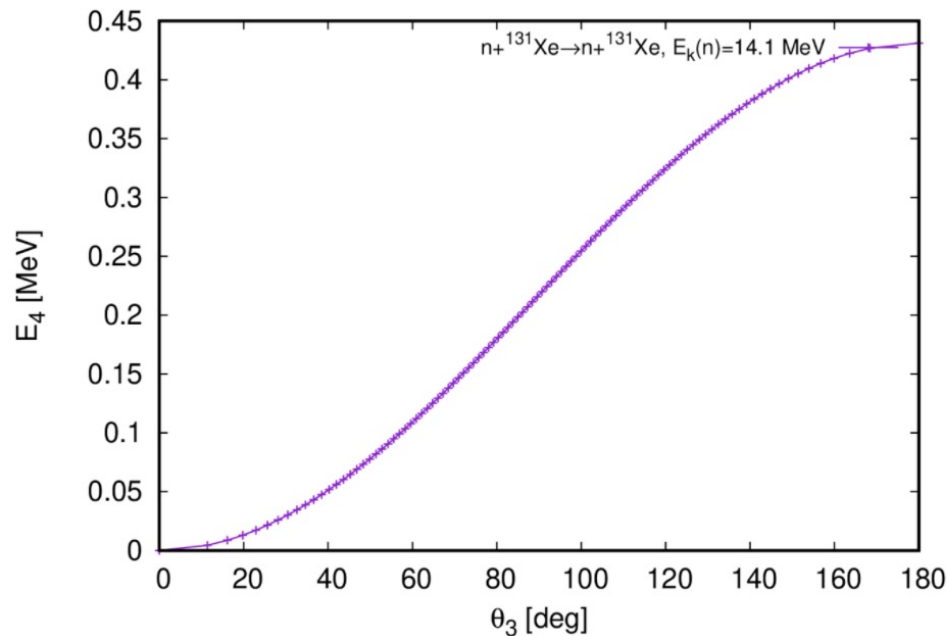
Neutron-Xenon elastic scattering spectrum

- Expected xenon recoil energies as a function of scattering angle
 - Energy endpoint at approximately 425 keV

Reaction summary for $n+^{131}\text{Xe}\rightarrow n+^{131}\text{Xe}$, $E_k(n)=14.1$ MeV

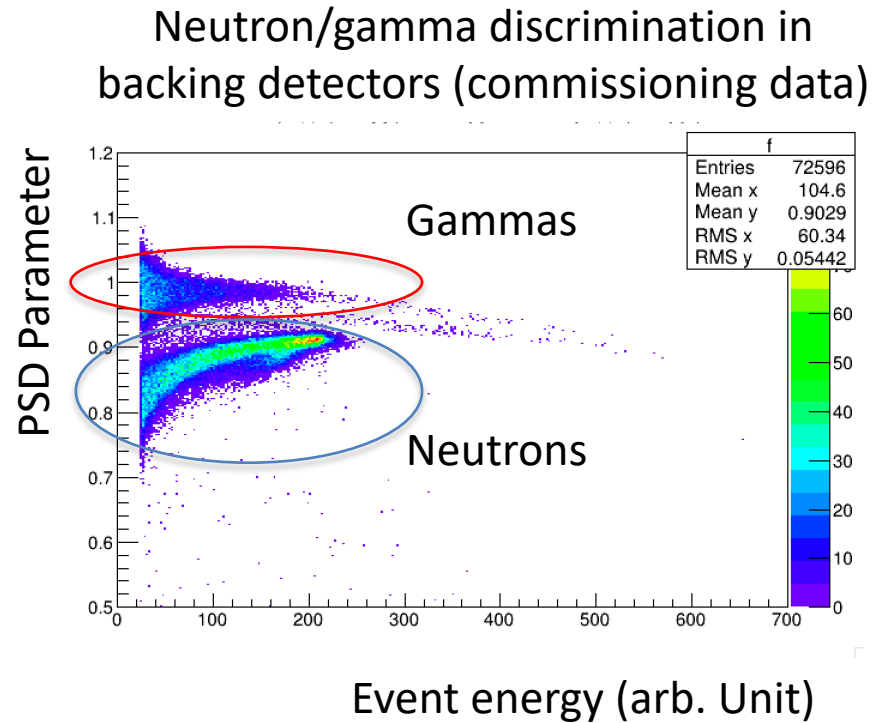
- The maximum n energy is 14.1 MeV. The minimum n energy is 13.669 MeV.
- The maximum ^{131}Xe energy is 0.431 MeV. The minimum ^{131}Xe energy is 0 MeV. The maximum ^{131}Xe angle is 90 degrees.

KE_4 as a function of θ_3 :



Selecting neutron candidate events

- Several handles for discriminating DT neutron events from backgrounds
 - S1/S2 ratio in Xenon TPC
 - Pulse discrimination in S1/S2 pulses
 - Pulse discrimination in backing detectors
 - Time-of-flight from Xenon TPC to backing detector
- Clear neutron/gamma separation apparent with PSD in backing detectors
- S1/S2 separation power with new reflector will be quantified prior to full data-taking run



Uncertainties in lowest recoil energy

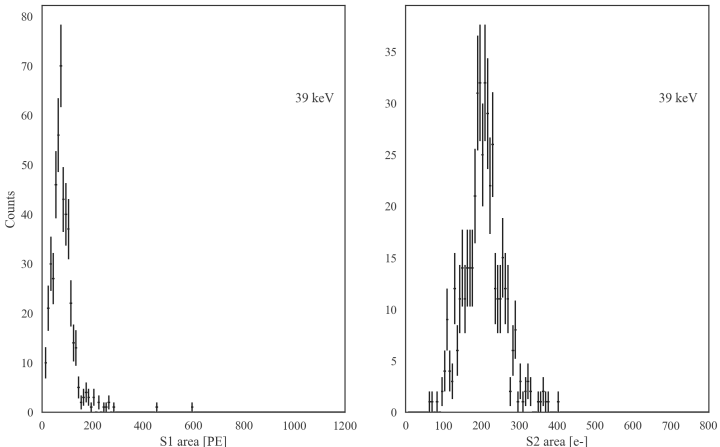
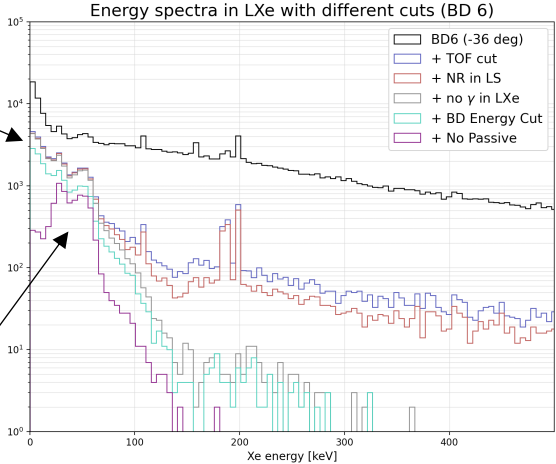
- Lowest recoil energy's Geant4-based model generally did not produce good fits to the detector data
 - Detector was placed at a peak in the inelastic scattering cross-section as predicted by Geant4
 - This corresponds to a trough in the elastic scattering cross-section, producing two-peak shape in simulation
 - Highly variable cross-section region, and current prediction in ENDF is calculated (not informed by DT data)
- Light/charge yield reported in paper instead evaluated assuming a Gaussian shape, with light/charge yield calculated directly
 - Difference in light/charge yield fits propagated as a systematic uncertainty in final results reported in table

Simulated energy distribution, lowest angle LS coincidence scatters

S1/S2 distributions, 2000 V/cm data, lowest angle LS coincidence scatters

Excess in low-energy scatters from passive materials

Dip in predicted ES cross-section results in two-hump feature



Excess in low-energy scatters in simulation

- Larger counts in low-energy scatters observed in simulation but not in data
- Excess appears associated with neutrons which undergo scatters in passive detector materials prior to scatter in xenon
 - Majority of scatters occur on PTFE or field rings
- Several possibilities for excess in simulation relative to data
 - Uncertainties in cross-section for DT neutrons on PTFE and copper in field ring

